Lycium barbarum polysaccharide attenuates alcoholic cellular injury through TXNIP-NLRP3 inflammasome pathway

Jia Xiao [a,d,e,#], Yinghui Zhu [b,#], Yingxia Liu [e], George L. Tipoe [d], Feiyue Xing [a,*], Kwok-Fai So [c,f,*]

[a] Department of Immunobiology, Institute of Tissue Transplantation and Immunology, Jinan University, Guangzhou 510632, China

[b] Sun Yat-sen University Cancer Center, State Key Laboratory of Oncology in South China, Guangzhou, China

[c] GMH Institute of CNS Regeneration, and Guangdong Medical Key Laboratory of Brain Function and Diseases, Jinan University, Guangzhou, China

[d] Department of Anatomy, The University of Hong Kong, Hong Kong, China

[e] Department of Infectious Diseases, Shenzhen Third People's Hospital, Shenzhen 518112, China

[f] Department of Ophthalmology, The University of Hong Kong, Hong Kong, China

[#] These authors contributed equally to this study.

[*] Corresponding authors. Tel.: +86 20 85220723 (F.Y. Xing) +86 20 85228362 (K.F. So).

E-mail address: tfyxing@jnu.edu.cn (F.Y. Xing) hrmaskf@hku.hk (K.F. So).

ABSTRACT

Lycium barbarum has been used as a traditional Chinese medicine to nourish liver, kidneys and the eyes. However, the underlying mechanisms of its hepatic-protective properties remain uncertain. In this study, we aimed to investigate whether thioredoxin-interacting protein (TXNIP) and NOD-like receptor 3 (NLRP3) inflammasome mediated the attenuation of ethanol-induced hepatic injury by *Lycium barbarum* polysaccharide (LBP). Rat normal hepatocyte line BRL-3A was pre-treated with LBP prior to ethanol incubation. Hepatic damages, including apoptosis, inflammation, and oxidative stress, were measured. Then the inhibition of endogenous TXNIP expression was achieved by using its specific siRNA to test its possible involvement in the injury attenuation. We found that 50 μg/ml LBP pre-treatment significantly alleviated 24-h ethanol exposure-induced overexpression of TXNIP, increased cellular apoptosis, secretion of inflammatory cytokines, activation of NLRP3 inflammasome, production of ROS, and reduced antioxidant enzyme expression. Silence of TXNIP suppressed the activated NLRP3 inflammasome, increased oxidative stress and worsened apoptosis in the cells. Further addition of LBP did not influence the effects of TXNIP inhibition on the cells. In conclusion, inhibition of hepatic TXNIP by LBP contributes to the reduction of cellular apoptosis, oxidative stress and NLRP3 inflammasome-mediated inflammation.

Keywords: LBP; TXNIP; NLRP3 inflammasome

1. Introduction

Alcoholic liver disease (ALD) encompasses a spectrum of hepatic injuries, ranging from steatosis to cirrhosis. The abuse of alcohol remains a major health and social burden all over the world. In the developed world, alcohol-related disease accounts for as much as 9.2% of all disability-adjusted life years [1]. Chronic over-consumption of alcohol induces steatosis, which occurs in more than 90% of heavy drinkers [2]. Advanced alcoholic fatty liver disease (steatohepatitis), fibrosis, and even hepatocellular carcinoma (HCC) may progress from prolonged alcohol consumption. To date, although several key events during the development of ALD have been identified, the detailed pathologic mechanisms of the disease and its interactions with other risk factors (e.g. age, obesity, and smoking) still remain elusive [3]. Among these characterized mechanisms, increased hepatic inflammation and oxidative stress are thought to play critical roles in the development of ALD [4, 5].

Inflammasomes are a group of large caspase-1-activating protein complexes in response to the evoke of innate immunity and production of pro-inflammatory cytokines, including NLRP3, NLRC4, AIM2 and NLRP6 inflammasomes [6]. They sense pathogen-associated molecular patterns (PAMPs) in the cytosol as well as the host-derived signals known as damage-associated molecular patterns (DAMPs) [7]. Inflammasomes, particularly NLRP3 inflammasome, are shown to be activated in a variety of liver diseases, including drug-induced liver injury [8], ischemia–reperfusion injury [9], endotoxin-induced liver injury and cholestasis [10, 11], viral hepatitis [12], fibrosis [13], and non-alcoholic fatty liver disease [14, 15]. However, to date, little is

known about the role of inflammasome in the pathogenesis of ALD.

Oxidative stress is another vital contributor to the development of ALD. It is shown that acute and chronic ethanol treatments increase the production of reactive oxygen and nitrogen species (ROS/RNS) while decrease cellular antioxidant defenses levels. Increased oxidative stress may cause lipid peroxidation, inflammation, apoptosis, and necrosis in the liver, forming a positive feedback loop which significantly aggravates the ALD severity [16]. One of the promoters of hepatic oxidative stress is thioredoxin-interacting protein (TXNIP), which can inhibit thioredoxins (Trx)-1 and -2 in the cytosol and mitochondria, respectively [17, 18]. TXNIP is found to be a promising therapeutic target in hepatic ischemia–reperfusion injury [19], hyperglycemia [20], acute liver failure [21], and HCC [22]. Interestingly, a recent study found that TXNIP links oxidative stress to inflammasome activation [23].

In clinic, treatment options for ALD are limited. Abstinence is the most important therapeutic intervention for patients. It has been demonstrated to significantly improve clinical outcomes and even to reverse fatty liver [24]. Nutritional support with herbal supplements receives mass attention in the past decade because this therapy is shown to reduce the severity of ALD both in basic studies and clinical trials [25]. In the current study, we firstly tested the protective effects of *lycium barbarum* polysaccharide (LBP), a proven hepatoprotective agent from Traditional Chinese medicine in an *in vitro* ALD model. The involvement of TXNIP and NLRP3 inflammasome were then characterized.

2. Materials and methods

2.1. Chemicals and reagents

The preparation for LBP extracts was the same as reported previously [26]. All cell culture consumables and reagents were bought from either Corning Incorporated (Corning, NY) or Gibco (Carlsbad, CA). Antibodies against catalase (CAT), glutathione peroxidase 1 (GPx1), NLRP3, and caspase-1 were bought from Abcam (Cambridge, England). ASC and TXNIP antibodies were purchased from Enzo Life Sciences (Farmingdale, NY) and Santa Cruz Biotechnology (Santa Cruz, CA), respectively. Pure ethanol was from Guangzhou Chemical Reagent Factory (Guangzhou, China).

2.2. Cell culture and treatments

Rat normal hepatocyte BRL-3A cell line was supplied by the Cell Bank of Type Culture Collection of Chinese Academy of Sciences (Shanghai, China). It was cultured in DMEM with 10% (v/v) FBS at 37 °C with 5% CO_2 using a cell incubator. Before every treatment, cells must reach a confluence of 60-70%. For the pre-treatment with LBP, PBS dissolved LBP was added 2 hours before the ethanol treatment.

For the small interfering RNA (siRNA) assay, BRL-3A cells were transiently transfected with 100 nM control siRNA or TXNIP siRNA (GenePharma, Shanghai, China) using Lipofectamine RNAiMAX (Invitrogen, Carlsbad, CA), according to the instructions from manufacturer [27]. After 48 hours, the efficiency of siRNA silencing

was measured by quantitative PCR. The sequences of TXNIP siRNA and PCR primers were listed in Table 1.

2.3. MTT assay

Cell viability was evaluated by the conversion of 3-(4,5-Dimethylthiazol-2-yl)-2,5-diphenyltetrazolium bromide (MTT, Sigma-Aldrich, St. Louis, MO) to a purple color product by cellular mitochondria. After drug treatment, cells from each group were washed by sterile PBS 3 times and then incubated with 5 mg/ml MTT for 3 hrs, and subsequently dissolved in dimethyl sulfoxide (DMSO). The absorbance of MTT was measured at 570 nm.

2.4. Quantification of apoptotic cells

After drug treatment, Hoechst 33342 (5 μg/ml) and propidium iodide (5 μg/ml) were added to each well to stain live cells. The results were expressed as the percentage of apoptosis (PA): PA = apoptotic cell number/ total cell number $\times$ 100% [28].

2.5. Measurement of ROS production

Intracellular production of ROS was detected by fluorescence probe 2',7'-dichlorofluorescin diacetate (DCFH-DA, Sigma-Aldrich) as previously described [29]. Briefly, after treatment, cells were washed three times with PBS and then incubated in 10 μM DCFH-DA for 30 min at 37 °C for green fluorescent light

visualization. Quantification of green fluorescence was analyzed by using ImageJ (Version 1.48, National Institutes of Health, Bethesda, MD).

2.6. RNA extraction and quantitative PCR

Total RNA of cells was extracted by using illustra™ RNAspin mini kit (GE healthcare, UK). The preparation of the first-strand cDNA was conducted following the instruction of the SuperScript™ First-Strand Synthesis System (Invitrogen, Calsbad, CA). The mRNA expression levels of target genes were measured by Takara SYBR premix Taq quantitative PCR system (Takara Bio Inc, Shiga, Japan) and in MyiQ2 real-time PCR machine (Bio-Rad). Parallel amplification of glyceraldehyde-3-phosphate dehydrogenase (GAPDH) was used as the internal control. Relative quantification was done by using the $2^{-\Delta\Delta Ct}$ method. The relative expression of the specific gene to the internal control was obtained and then expressed as percentage of the control value. All real-time PCR procedures including the design of primers, validation of PCR environment and quantification methods were performed according the MIQE guideline [30].

2.7. Western blot

Western blot analyses of cell lysates were performed as described [31]. The ratio of the optical density of the protein product to the internal control (β-actin) was obtained and was expressed as ratio or percentage of the control value in the Figures.

2.8. ELISA assay

ELISA measurements of secreted TNF-α, IL-1β, and IL-6 were performed by using corresponding ELISA development kits from PeproTech (PeproTech Inc., Rocky Hill, NJ) according to user instructions. ELISA assay kit for secreted IL-18 was purchased from Invitrogen.

2.9. Statistical analysis

Data from each group were expressed as means $\pm$ SEM. Statistical comparison between groups was done using the Kruskal–Wallis test followed by Dunn's post hoc test to detect differences in all groups. A $p < 0.05$ was considered to be statistically significant (Prism 5.0, Graphpad software, Inc., San Diego, CA).

3. Results

3.1. LBP alleviated cellular injury, apoptosis, inflammation and oxidative stress in BRL-3A cells

After 24 and 48 hrs incubation with ethanol, the viability of BRL-3A cells decreased in a dose-dependent manner. However, there was a significant change between control and ethanol-treated group only when the dose of ethanol was higher than 50 mM (Figs. 1A and 1B). Interestingly, the decreasing levels of each ethanol dose between 24-hr and 48-hr treatment were quite similar, indicating that the damaging effects of ethanol on BRL-3A cells primarily occurred in the first 24 hrs (Figs. 1A and 1B). Therefore, in order to induce evident alcoholic cellular injury, we chose 250 mM as the treatment dose and 24 hrs as the duration in the following experiments.

To find out the optimal dose of LBP treatment, different doses (0 - 500 μg/ml) prior to the ethanol incubation were applied. Results showed that 50, 100, and 500 μg/ml of LBP recovered the cell viability to control-comparable levels (Fig. 1C). Thus, we selected 50 μg/ml as the treating dose of LBP in the following studies.

Since apoptosis is a direct consequence of ethanol-induced hepatic damage, we firstly measured the change of BRL-3A cellular apoptotic ratio after ethanol exposure in the absence or presence of LBP pre-treatment. It was exhibited that ethanol incubation significantly increased the apoptotic ratio from ~3% to ~25% ($p < 0.05$), which was attenuated by the LBP treatment (from ~25% to ~18%, $p < 0.05$). Vehicle LBP treatment did not influence the cell apoptosis (Fig. 1D). Then we measured the

secretion protein level of pro-inflammatory cytokines TNF-α and IL-6 in the medium. Similar to the change of apoptotic ratio, ethanol significantly increased the secretion of both TNF-α and IL-6 from BRL-3A cells, indicating an inflammatory status of the cells (Figs. 1E and 1F). Pre-treatment with LBP reduced the cytokine levels without influencing their basal secretions (Figs. 1E and 1F).

To further investigate the involvement of oxidative stress in the ethanol-induced damage, we stained the production of cellular ROS after ethanol incubation with or without LBP pre-treatment. It was found that ethanol obviously increased the signal of ROS staining, while LBP slightly reduced it (Fig. 1G). This phenomenon was in line with the antioxidant enzymes' result, in which the cellular level of CAT and GPx1 was significantly down-regulated by ethanol incubation but recovered by the pre-treatment with LBP (Figs. 1H and 1I). We also found that the cellular protein level of TXNIP was positively correlated with the production of ROS (Fig. 1J). All these data indicated that pre-treatment with 50 μg/ml LBP attenuated ethanol-induced cellular injury, apoptosis, inflammation and oxidative stress in BRL-3A cells.

* Figure 1 here *

3.2. LBP inhibited NLRP3 inflammasome activation after ethanol exposure

To characterize the involvement of NLRP3 in ethanol-induced hepatocyte damage and LBP-mediated protection, secreted protein levels of both IL-1β and IL-18 were measured by ELISA in all groups. It was shown that ethanol significantly

increased the secretion of both proteins and LBP counteracted such effects without affecting their basal levels (Figs. 2A and 2B). Then the cellular contents of key NLRP3 inflammasome components, including NLRP3, ASC and caspase-1 were examined by Western blot. Results exhibited that 24-hr ethanol incubation significantly up-regulated their protein levels, indicating that NLRP3 inflammasome was activated during ethanol incubation (Figs. 2C-2E). Pre-treatment with LBP significantly reduced their levels (Figs. 2C-2E).

* Figure 2 here *

3.3. LBP alleviated NLRP3 inflammasome in a TXNIP-dependent manner

To verify that the inhibition of NLRP3 inflammasome was due to the down-regulation of TXNIP, BRL-3A cells were transfected with TXNIP siRNA for 48 hrs and then incubated with ethanol and/or LBP. We found that siRNA against TXNIP successfully inhibited its endogenous expression, verified by quantitative PCR assay (Fig. 3A). TXNIP silencing prevented ethanol-induced cellular apoptosis, TNF-α, and ROS production in BRL-3A cells, indicating that hepatic TXNIP may mediate the activation of cellular injury pathways in ethanol-exposed cells (Figs. 3B-3D). Addition of LBP did not pose further influence in this cell model (Figs. 3B-3D). Control siRNA did not influence the cellular phenotypes affected by ethanol (data not shown).

* Figure 3 here *

Then the secretion of IL-1β and IL-18, as well as the cellular protein content of NLRP-3, ASC and caspase-1 were measured. Consistent with the change of apoptotic ratio and TNF-α secretion, inhibition of TXNIP significantly decreased the elevated contents, either cellular or secreted, of all these proteins after ethanol exposure. Pre-treated LBP prior to ethanol incubation did not further affect the effects of TXNIP on these markers (Fig. 4). These data confirmed that TXNIP mediated the amelioration of hepatic injury by LBP pre-treatment under ethanol-exposure condition.

* Figure 4 here *

4. Discussion

The hepatoprotective roles of LBP have been extensively studied in the past decade. In chemical-induced acute liver injury model and high-fat diet-induced NAFLD model, LBP is shown to attenuate hepatic disorders, including histological changes, lipid deposition, oxidative stress, inflammation, and apoptosis [32, 33]. For ALD, only one study indicating that, in a rat AFLD model, co-treatment with 300 mg/kg LBP significantly ameliorated liver injury, prevented the progression of alcohol-induced fatty liver, and improved the antioxidant functions when compared with the ethanol group [34]. However, the detailed protective mechanisms were still unknown. Here we firstly showed that pre-treatment with 50 μg/ml LBP significantly attenuated ethanol-induced hepatocyte damages, including cell death, apoptosis, inflammation and oxidative stress. Then the involvement of TXNIP and NLRP3 inflammasome in the protection of LBP against ethanol was demonstrated, which was consistent with its potent antioxidant and anti-inflammatory properties reported by previous studies [35, 36].

To date, little is known about the role of NLRP3 inflammasome in ALD. It is already documented that serum levels of IL-1β were increased in both alcoholics and experimental animal model [37, 38]. Also, in HepG2 cells treated with acetaldehyde, a metabolic product of alcohol, the secretion level of both IL-1β and TNF-α was increased [39]. Recently, in a mouse model of chronic alcohol feeding, activated NLRP3 inflammasome components (NLRP3, ASC, and pro-caspase-1) as well as increased serum and liver mature IL-1β were observed, suggesting that inflammasome

activation is an pathogenic event in ALD [40]. In this study, we demonstrated that after ethanol incubation, the secretion of pro-inflammatory cytokines was increased in parallel with the activation of NLRP3 inflammasome, further confirmed the involvement of this kind of inflammasome in ethanol-induced hepatic injury. Addition of LBP counteracted such effects from ethanol.

As (1) oxidative damage is an event predominantly in hepatocytes following alcohol administration and (2) increased oxidative stress may promote cellular inflammation and apoptosis, applying antioxidant compounds to protect against the liver injury is rational [41]. Under hyperglycemia, over-expressed TXNIP switches the function of TXNIP from TRX repressor to NLRP3 inflammasome activator [42]. Recently, TXNIP was further confirmed to directly activate NLRP3 inflammasome upon oxidative stress [23]. In addition, activated NLRP3 induces caspase-1 hyperactivity, which cleaved the precursor forms of IL-1β and IL-18 to increase the inflammatory responses in the liver [43]. Therefore, regulating the expression of TXNIP may be an effective way to inhibit the hepatic inflammation through attenuating NLRP3 activation. In the current *in vitro* study, LBP administration significantly reduced the expression NLRP3 inflammasome complex and ROS production upon ethanol exposure. Silence of endogenous TXNIP expression blocked those events, as well as hepatic injuries including apoptosis and oxidative stress, confirming the essential role of TXNIP in the induction of NLRP3 inflammasome and the possible mechanistic pathway of LBP protection.

In conclusion, LBP attenuated ethanol-induced hepatic damages through

suppressing the activation of NLRP3 inflammasome in a TXNIP-dependent manner in the BRL-3A *in vitro* system. These results further supported evidence that inhibition of hepatic TXNIP-NLRP3 inflammasome axis contributes to the alleviation of hepatic injury caused by ethanol. This axis may provide a novel therapeutic target of ALD.

Conflict of interest

All authors have approved the final manuscript and the authors declare that they have no conflicts of interest to disclose.

References

[1] WorldHealthOrganization, (2011).

[2] R.S. O'Shea, S. Dasarathy, A.J. McCullough, Hepatology (Baltimore, Md.), 51 (2010) 307-328.

[3] B. Gao, R. Bataller, Gastroenterology, 141 (2011) 1572-1585.

[4] A. Dey, A.I. Cederbaum, Hepatology (Baltimore, Md.), 43 (2006) S63-74.

[5] A.T. Duddempudi, Clinics in liver disease, 16 (2012) 687-698.

[6] M. Lamkanfi, V.M. Dixit, Annual review of cell and developmental biology, 28 (2012) 137-161.

[7] K. Schroder, J. Tschopp, Cell, 140 (2010) 821-832.

[8] A.B. Imaeda, A. Watanabe, M.A. Sohail, S. Mahmood, M. Mohamadnejad, F.S. Sutterwala, R.A. Flavell, W.Z. Mehal, The Journal of clinical investigation, 119 (2009) 305-314.

[9] D. Takeuchi, H. Yoshidome, A. Kato, H. Ito, F. Kimura, H. Shimizu, M. Ohtsuka, Y. Morita, M. Miyazaki, Hepatology (Baltimore, Md.), 39 (2004) 699-710.

[10] F.G. Bauernfeind, G. Horvath, A. Stutz, E.S. Alnemri, K. MacDonald, D. Speert, T. Fernandes-Alnemri, J. Wu, B.G. Monks, K.A. Fitzgerald, V. Hornung, E. Latz, Journal of immunology (Baltimore, Md. : 1950), 183 (2009) 787-791.

[11] M. Ganz, T. Csak, B. Nath, G. Szabo, World journal of gastroenterology : WJG, 17 (2011) 4772-4778.

[12] D. Burdette, A. Haskett, L. Presser, S. McRae, J. Iqbal, G. Waris, The Journal of general virology, 93 (2012) 235-246.

[13] A. Watanabe, M.A. Sohail, D.A. Gomes, A. Hashmi, J. Nagata, F.S. Sutterwala, S. Mahmood, M.N. Jhandier, Y. Shi, R.A. Flavell, W.Z. Mehal, American journal of physiology. Gastrointestinal and liver physiology, 296 (2009) G1248-1257.

[14] T. Csak, M. Ganz, J. Pespisa, K. Kodys, A. Dolganiuc, G. Szabo, Hepatology (Baltimore, Md.), 54 (2011) 133-144.

[15] B. Vandanmagsar, Y.H. Youm, A. Ravussin, J.E. Galgani, K. Stadler, R.L. Mynatt, E. Ravussin, J.M. Stephens, V.D. Dixit, Nature medicine, 17 (2011) 179-188.

[16] J.I. Beier, C.J. McClain, Biological chemistry, 391 (2010) 1249-1264.

[17] P.C. Schulze, J. Yoshioka, T. Takahashi, Z. He, G.L. King, R.T. Lee, The Journal of biological chemistry, 279 (2004) 30369-30374.

[18] P. Patwari, L.J. Higgins, W.A. Chutkow, J. Yoshioka, R.T. Lee, The Journal of biological chemistry, 281 (2006) 21884-21891.

[19] V. Nivet-Antoine, C.H. Cottart, H. Lemarechal, M. Vamy, I. Margaill, J.L. Beaudeux, D. Bonnefont-Rousselot, D. Borderie, Biochimie, 92 (2010) 1766-1771.

[20] W.A. Chutkow, P. Patwari, J. Yoshioka, R.T. Lee, The Journal of biological chemistry, 283 (2008) 2397-2406.

[21] S.J. Kim, S.M. Lee, Free radical biology & medicine, 65 (2013) 997-1004.

[22] F. Yamaguchi, Y. Hirata, H. Akram, K. Kamitori, Y. Dong, L. Sui, M. Tokuda, BMC cancer, 13 (2013) 468.

[23] R. Zhou, A. Tardivel, B. Thorens, I. Choi, J. Tschopp, Nature immunology, 11 (2010) 136-140.

[24] F. Pessione, M.J. Ramond, L. Peters, B.N. Pham, P. Batel, B. Rueff, D.C. Valla, Liver international : official journal of the International Association for the Study of the Liver, 23 (2003) 45-53.

[25] T.H. Frazier, A.M. Stocker, N.A. Kershner, L.S. Marsano, C.J. McClain, Therapeutic advances in

gastroenterology, 4 (2011) 63-81.

[26] M.S. Yu, S.K. Leung, S.W. Lai, C.M. Che, S.Y. Zee, K.F. So, W.H. Yuen, R.C. Chang, Experimental gerontology, 40 (2005) 716-727.

[27] W. Wang, C. Wang, X.Q. Ding, Y. Pan, T.T. Gu, M.X. Wang, Y.L. Liu, F.M. Wang, S.J. Wang, L.D. Kong, British journal of pharmacology, 169 (2013) 1352-1371.

[28] J. Xiao, Z.C. Zhou, C. Chen, W.L. Huo, Z.X. Yin, S.P. Weng, S.M. Chan, X.Q. Yu, J.G. He, Molecular immunology, 44 (2007) 3615-3622.

[29] Y.K. Lee, J.T. Hwang, D.Y. Kwon, Y.J. Surh, O.J. Park, Cancer letters, 292 (2010) 228-236.

[30] S.A. Bustin, V. Benes, J.A. Garson, J. Hellemans, J. Huggett, M. Kubista, R. Mueller, T. Nolan, M.W. Pfaffl, G.L. Shipley, J. Vandesompele, C.T. Wittwer, Clinical chemistry, 55 (2009) 611-622.

[31] J. Xiao, Y.P. Ching, E.C. Liong, A.A. Nanji, M.L. Fung, G.L. Tipoe, European journal of nutrition, 52 (2013) 179-191.

[32] J. Xiao, E.C. Liong, Y.P. Ching, R.C. Chang, K.F. So, M.L. Fung, G.L. Tipoe, Journal of ethnopharmacology, 139 (2012) 462-470.

[33] J. Xiao, E.C. Liong, Y.P. Ching, R.C. Chang, M.L. Fung, A.M. Xu, K.F. So, G.L. Tipoe, Nutrition & diabetes, 3 (2013) e81.

[34] D. Cheng, H. Kong, Molecules (Basel, Switzerland), 16 (2011) 2542-2550.

[35] M. Jin, Q. Huang, K. Zhao, P. Shang, International journal of biological macromolecules, 54 (2013) 16-23.

[36] H. Li, Y. Liang, K. Chiu, Q. Yuan, B. Lin, R.C. Chang, K.F. So, PloS one, 8 (2013) e68881.

[37] C.J. McClain, D.A. Cohen, C.A. Dinarello, J.G. Cannon, S.I. Shedlofsky, A.M. Kaplan, Life sciences, 39 (1986) 1479-1485.

[38] S.L. Valles, A.M. Blanco, I. Azorin, R. Guasch, M. Pascual, M.J. Gomez-Lechon, J. Renau-Piqueras, C. Guerri, Alcoholism, clinical and experimental research, 27 (2003) 1979-1986.

[39] C.Y. Hsiang, S.L. Wu, S.E. Cheng, T.Y. Ho, Journal of biomedical science, 12 (2005) 791-801.

[40] J. Petrasek, S. Bala, T. Csak, D. Lippai, K. Kodys, V. Menashy, M. Barrieau, S.Y. Min, E.A. Kurt-Jones, G. Szabo, The Journal of clinical investigation, 122 (2012) 3476-3489.

[41] A. Ambade, P. Mandrekar, International journal of hepatology, 2012 (2012) 853175.

[42] K. Schroder, R. Zhou, J. Tschopp, Science (New York, N.Y.), 327 (2010) 296-300.

[43] J. Tschopp, K. Schroder, Nature reviews. Immunology, 10 (2010) 210-215.

Figure legends

Fig. 1. Effects of LBP on ethanol-induced hepatic injury. (A, B) BRL-3A cells were treated by 0, 1, 10, 50, 100, 250, 500 and 1000 mM ethanol for 24 hrs or 48 hrs. Cell viability after ethanol exposure was measured by MTT assay. (C) BRL-3A cells were treated by 250 mM with pre-treatment with 0, 1, 10, 50, 100 and 500 μg/ml LBP for 24 hrs. Cell viability after ethanol exposure was measured by MTT assay. To test the effects of LBP on 24-hr ethanol-induced hepatic apoptosis and inflammation, (D) apoptotic ratio, (E) secreted TNF-α content, and (F) secreted IL-6 content were measured by Hoechst 33342/propidium iodide and ELISA, respectively. (G) The panel shows the fluorescent image stained DCFH-DA for the measurement of ROS production in BRL-3A cells (magnification, x200). Quantified green fluorescence values were analyzed by ImageJ. To verify the oxidative stress change after LBP and ethanol treatments, protein expression of (H) CAT, (I) GPx1, and (J) TXNIP was measured by Western blot. Data from each group (n = 5) were expressed as means ± SEM. Statistical comparison between groups was done using the Kruskal–Wallis test followed by Dunn's post hoc test to detect differences in all groups. A $p < 0.05$ was considered to be statistically significant and showed as different letters (e.g. a and b). EtOH, ethanol; v-LBP, vehicle LBP; E+L, ethanol with LBP pre-treatment.

Fig. 2. Effects of 50 μg/ml LBP on 24-hr ethanol-induced activation of NLRP3 inflammasome. Change of secreted protein content of (A) IL-1β and (B) IL-18 was

measured by ELISA in BRL-3A cells. Then the change of protein level of (C) NLRP3, (D) ASC, and (E) caspase-1 was measured by Western blot in BRL-3A cells. Data from each group (n = 5) were expressed as means ±SEM. Statistical comparison between groups was done using the Kruskal–Wallis test followed by Dunn's post hoc test to detect differences in all groups. A $p < 0.05$ was considered to be statistically significant and showed as different letters (e.g. a and b). EtOH, ethanol; v-LBP, vehicle LBP; E+L, ethanol with LBP pre-treatment.

Fig. 3. Influence of TXNIP silence on 24-hr ethanol-induced hepatic apoptosis, inflammation and ROS production in BRL-3A cells. (A) The panel shows the efficiency of siRNA against TXNIP, when compared with the control siRNA, on endogenous TXNIP mRNA expression. Then the change of (B) apoptotic ratio, (C) secreted TNF-α content, and (D) ROS production was measured by Hoechst 33342/propidium iodide, ELISA, and DCFH-DA staining (magnification, x200), respectively. Quantified green fluorescence values were analyzed by ImageJ. Data from each group (n = 5) were expressed as means ±SEM. Statistical comparison between groups was done using the Kruskal–Wallis test followed by Dunn's post hoc test to detect differences in all groups. A $p < 0.05$ was considered to be statistically significant and showed as different letters (e.g. a and b).

Fig. 4. Influence of TXNIP silence on 24-hr ethanol-induced activation of NLRP3 inflammasome. Change of secreted protein content of (A) IL-1β and (B) IL-18 was

measured by ELISA in BRL-3A cells. Then the change of protein level of (C) NLRP3, (D) ASC, and (E) caspase-1 was measured by Western blot in BRL-3A cells. Data from each group (n = 5) were expressed as means $\pm$ SEM. Statistical comparison between groups was done using the Kruskal–Wallis test followed by Dunn's post hoc test to detect differences in all groups. A $p < 0.05$ was considered to be statistically significant and showed as different letters (e.g. a and b).

A

B

C

NLRP3

Actin

D

ASC

Actin

E

caspase-1

Actin

A

TXNIP mRNA(%Ctrl)

siRNA-control (100 nM)	+	-
siRNA-TXNIP (100 nM)	-	+

B

Apoptosis Ratio (%)

Ethanol (250 mM)	-	+	+	+
siRNA-control (100 nM)	-	+	-	-
siRNA-TXNIP (100 nM)	-	-	+	+
LBP (50 µg/ml)	-	-	-	+

C

TNF-α secretion (%Ctrl)

Ethanol (250 mM)	-	+	+	+
siRNA-control (100 nM)	-	+	-	-
siRNA-TXNIP (100 nM)	-	-	+	+
LBP (50 µg/ml)	-	-	-	+

D

Ethanol (250 mM)	-	+	+	+
siRNA-control (100 nM)	-	+	-	-
siRNA-TXNIP (100 nM)	-	-	+	+
LBP (50 µg/ml)	-	-	-	+

Green Fluorescence (RFU)

Ethanol
Ethanol+siRNA-control
Ethanol+siRNA-TXNIP
Ethanol+siRNA-TXNIP+LBP

A

Ethanol (250 mM)   -   +   +   +
siRNA-control (100 nM) -   +   -   -
siRNA-TXNIP (100 nM) -   -   +   +
LBP (50 µg/ml)   -   -   -   +

B

Ethanol (250 mM)   -   +   +   +
siRNA-control (100 nM) -   +   -   -
siRNA-TXNIP (100 nM) -   -   +   +
LBP (50 µg/ml)   -   -   -   +

C

Ethanol (250 mM)   -   +   +   +
siRNA-control (100 nM) -   +   -   -
siRNA-TXNIP (100 nM) -   -   +   +
LBP (50 µg/ml)   -   -   -   +

D

Ethanol (250 mM)   -   +   +   +
siRNA-control (100 nM) -   +   -   -
siRNA-TXNIP (100 nM) -   -   +   +
LBP (50 µg/ml)   -   -   -   +

E

Ethanol (250 mM)   -   +   +   +
siRNA-control (100 nM) -   +   -   -
siRNA-TXNIP (100 nM) -   -   +   +
LBP (50 µg/ml)   -   -   -   +
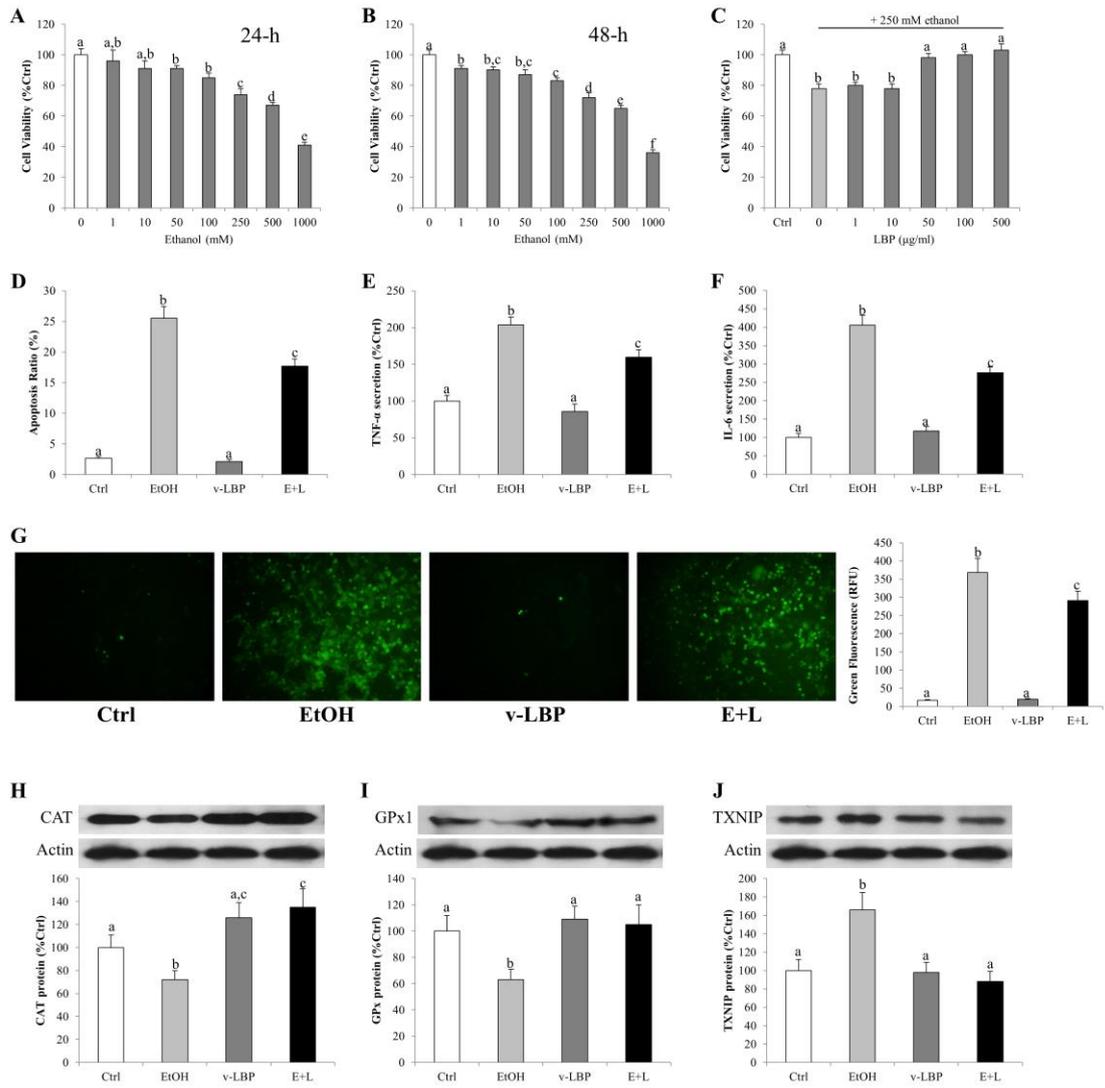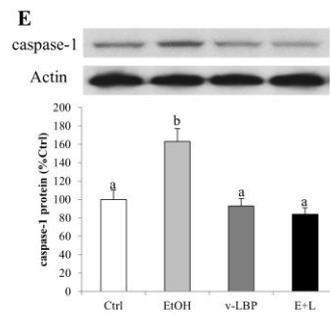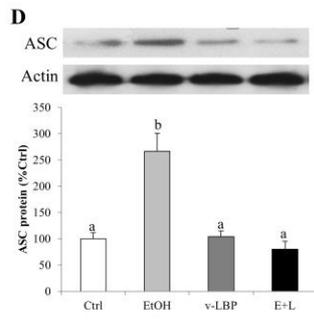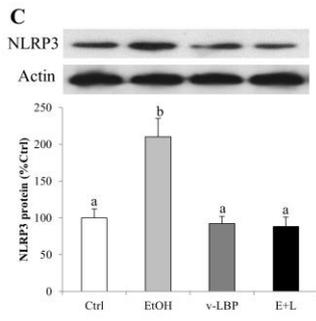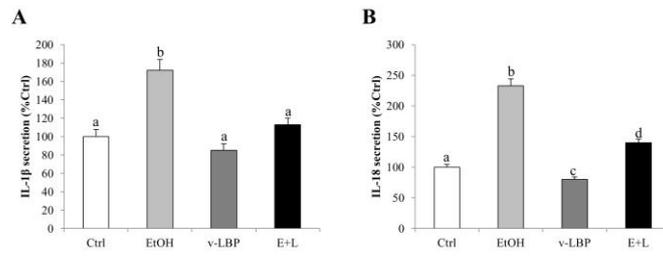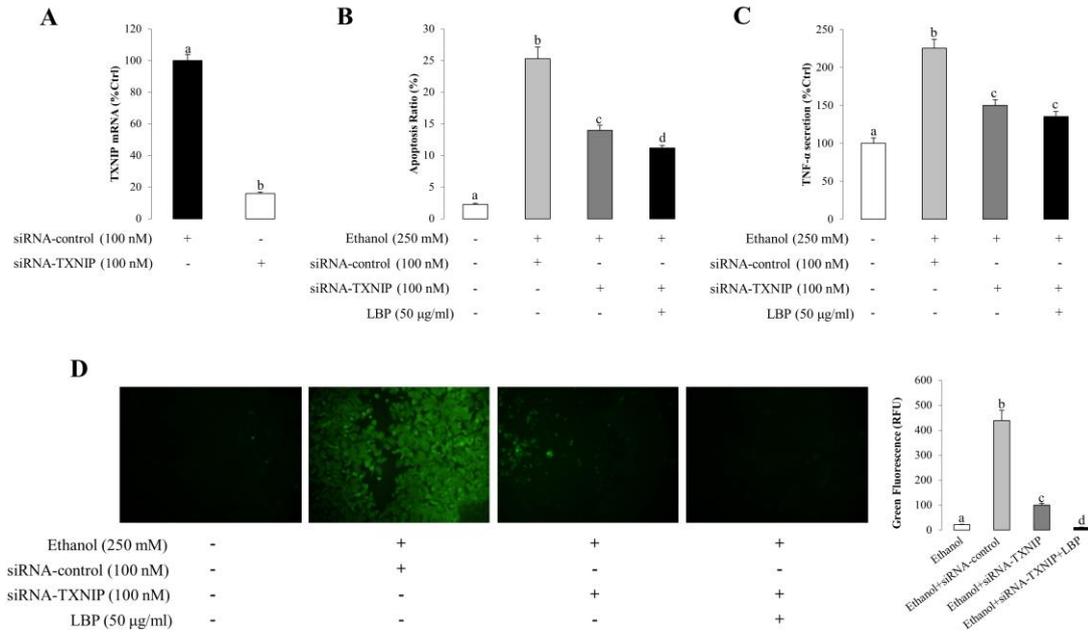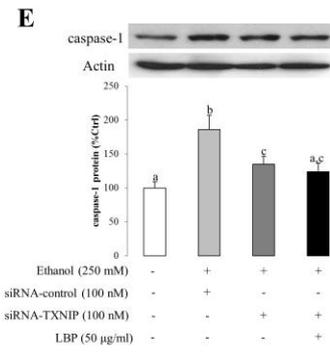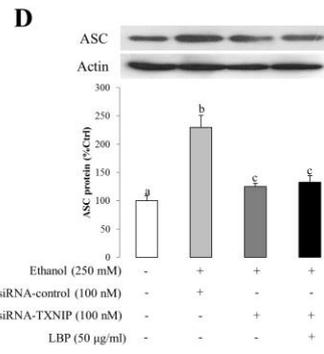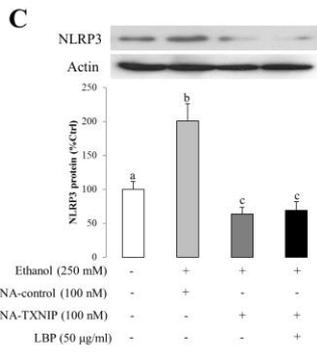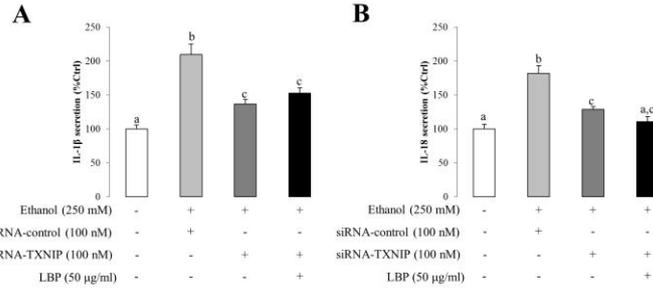
Table 1. Sequences of TXNIP siRNA and PCR primers.

Name	Sequence
Rat TXNIP siRNA	s: 5'-GCUGGAUAGACCUAAACAUTT-3'
	as: 5'-AUGUUUAGGUCUAUCCAGCTT-3'
Control siRNA	s: 5'-UUCUCCGAACGUGUCACGUTT-3'
	as: 5'-ACGUGACACGUUCGGAGAATT-3'
Rat TXNIP mRNA	s: 5'-TAGTGTCCCTGGCTCCAAGAAA-3'
	as: 5'-GGATGTTTAGGTCTATCCAGCTCAT-3'
Rat GAPDH	s: 5'-AGGTCGGTGTGAACGGATTTG-3'
	as: 5'-TGTAGACCATGTAGTTGAGGTCA-3'